2013 Hawaii University International Conferences
Education & Technology
Math & Engineering Technology
June 10th to June 12th
Ala Moana Hotel
Honolulu, Hawaii

Steady-State Viscoelastic Rimming Flow

Sergei Fomin
California State University, Chico, Chico, CA
R. Shankar
Butte College, Oroville, CA
N. Danes
California State University, Bakersfield, Bakersfield, CA
A. Yasuda
University of California, Riverside, Riverside, CA
D. Costo
California State University, Sacramento, Sacramento, CA

Title:

Steady-State Viscoelastic Rimming Flow

Name of authors: ,

R. Shankar[2]**, N. Danes**[3]**, A. Yasuda**[4]**, D. Costo**[5]**, Sergei Fomin**[1]

Department and Affiliation/University

[1]*Department of Mathematics and Statistics, California State University, Chico, Chico, CA*

[2]*Department of Chemistry, Butte College, Oroville, CA*
[3]*Department of Mathematics, California State University, Bakersfield, Bakersfield, CA*
[4]*Department of Mathematics, University of California, Riverside, Riverside, CA*
[5]*Department of Mathematics, California State University, Sacramento, Sacramento, CA*

Steady-State Viscoelastic Rimming Flow

R. Shankar[2], N. Danes[3], A. Yasuda[4], D. Costo[5], S. Fomin[1]

[1]*Department of Mathematics and Statistics, California State University, Chico, Chico, CA*

[2]*Department of Chemistry, Butte College, Oroville, CA*

[3]*Department of Mathematics, California State University, Bakersfield, Bakersfield, CA*

[4]*Department of Mathematics, University of California, Riverside, Riverside, CA*

[5]*Department of Mathematics, California State University, Sacramento, Sacramento, CA*

Abstract

Using scale analysis and asymptotic expansion, a theoretical description is obtained for the non-Newtonian viscoelastic flow on the inner wall of a rotating horizontal cylinder. The Oldroyd-B constitutive equation is chosen to model the viscoelastic properties of the fluid. In the general case, the governing equations can only be solved numerically. However, since the polymeric solutes used in roto-molding and coating technologies exhibit relatively weak elastic properties, the Deborah number for such flows is small ($De < 1$). Exploiting this fact, asymptotic expansion is applied to simplify the model. The nonlinear partial differential equations for the thickness of the fluid film are derived. For the steady-state case, an approximate analytical solution is obtained.

1. Introduction

The problem of rotational flow on the inner and/or outer wall of a hollow horizontal cylinder has been of interest for many years due to its wide range of applications in industry [1, 2]. Moffatt [3] was the first to derive the condition of the maximal supportable load for a Newtonian liquid. Later, Preziosi & Joseph [4] presented the same condition in another form and named it a run-off condition for coating and rimming flows. The possible instability of the liquid film on a cylindrical surface is one the most fundamentally challenging aspects of this problem. The highly unstable nature of Newtonian rimming flow was discussed in a number of recent publications [5-10]. Benilov and O'Brien [5] and Benilov [6] examined the stability of the solutions, accounting for inertial forces and surface tension, and concluded that including higher order corrections to the governing equations for the liquid film thickness may cause the instability of the steady-state solution. They proved that while inertia always causes instability, viscosity can make the characteristic time of growth large enough to effectively stabilize the film. Benilov et al [7, 8] have shown that the system admits strongly unstable solutions, which develop singularities in a finite time. Although the aforementioned investigations highlight the main characteristics of rimming flow, not enough has been done to show the effect of non-Newtonian properties on such flow, both in the cases of steady and non-steady flow. Only a few attempts have been made, in which the power-law model [11, 12], Carrea-Yasuda model [13, 14], Ellis model [15], and Bingham model [16] were used. The viscoelastic rimming flow and corresponding numerical solutions for were studied in [17] and [18]. Most polymeric solutes

used in rotational coating are non-Newtonian liquids, which exhibit moderate elastic behavior characterized by the Deborah number $De = \lambda_1 \Omega$, where Ω is the characteristic angular velocity of the rotating cylinder, and λ_1 is the typical liquid polymer relaxation time. The values of the Deborah number are well documented [18-20] and normally stay in the range from 10^{-2} to 10^{-1}. Our main concern is the rotational molding of highly viscous polymers [1, 2] that exhibit non-Newtonian viscoelastic behavior. We are particularly interested in eliminating possible instabilities and providing the criteria for a continuous and smooth coating film on the wall of the horizontal rotating cylinder. In the present study of the rimming flow of viscoelastic non-Newtonian fluids, the governing equations are analyzed analytically and numerically.

2. System Model and Scale Analysis

A schematic sketch of the rimming flow is illustrated in **Fig. 1**. The cylinder of radius r_0 is rotating in the counterclockwise direction with constant angular velocity Ω. The horizontal cylinder is assumed to be of infinite length and open. A highly viscous liquid layer covers the inner wall of the cylinder and moves along this wall by the actions of viscous and gravitational forces. The rest of the cylinder volume is occupied by relatively rarefied gas, which exerts negligible viscous traction at the gas–liquid interface and is consequently modeled with a given uniform pressure. A cylindrical system of coordinates (r, z, θ) is implemented such that the z-axis coincides with the axis of the cylinder. It is assumed that the cylinder is infinitely long, so that the flow is two-dimensional. Since it is well documented [3, 13, 14] that rimming flow is dominated by the interaction of gravitational and viscous forces and that the effect of inertial forces is negligibly small, the conservation laws for the mass and momentum of an incompressible fluid can be presented in the following vector form:

$$\frac{\partial \rho}{\partial t^*} + \nabla^* \cdot \rho \mathbf{v}^* = 0 . \tag{1}$$

$$\rho \mathbf{g} - \nabla^* p^* + \nabla^* \cdot \boldsymbol{\tau}^* = \rho \frac{D\mathbf{v}^*}{Dt^*}, \tag{2}$$

The constitutive equation for an Oldroyd-B fluid can be written as [21]

$$\begin{aligned} &\boldsymbol{\tau}^* + \lambda_1 \left(\frac{\partial \boldsymbol{\tau}^*}{\partial t} + \left\{ \mathbf{v}^* \bullet \nabla^* \boldsymbol{\tau}^* \right\} - \left(\left(\nabla^* \mathbf{v}^* \right)^{\mathrm{T}} \bullet \boldsymbol{\tau}^* \right) - \left(\left(\nabla^* \mathbf{v}^* \right)^{\mathrm{T}} \bullet \boldsymbol{\tau}^* \right)^{\mathrm{T}} \right) = \\ &2\mu \left(\mathbf{D}^* + \lambda_2 \left(\frac{\partial \mathbf{D}^*}{\partial t} + \left\{ \mathbf{v}^* \bullet \nabla^* \mathbf{D}^* \right\} - \left(\left(\nabla^* \mathbf{v}^* \right)^{\mathrm{T}} \bullet \mathbf{D}^* \right) - \left(\left(\nabla^* \mathbf{D}^* \right)^{\mathrm{T}} \bullet \mathbf{D}^* \right)^{\mathrm{T}} \right) \right), \end{aligned} \tag{3}$$

where $\boldsymbol{\tau}^*$ is the stress tensor, $\mathbf{D}$ is the deformation rate tensor, μ is the total viscosity composed of solvent and polymer components respectively, $\mu = \mu_s + \mu_p$, λ_1 is the fluid relaxation time, λ_2 is the retardation time:

$$\lambda_2 = K \cdot \lambda_1, \tag{3.1}$$

and K is the ratio of the solvent viscosity to the solution viscosity,

$$K = \frac{\mu_s}{\mu}. \tag{3.2}$$

Boundary conditions on the free surface are as follows:

$$-p^* + \mathbf{n}\cdot\boldsymbol{\tau}^*\cdot\mathbf{n} = 2\kappa\sigma, \qquad \mathbf{n}\cdot\boldsymbol{\tau}^*\cdot\mathbf{t} = 0, \tag{4}$$

where **n** is the normal unit vector external to the liquid layer, **t** is the unit tangent vector, σ is the surface tension, and κ is the mean curvature of the free surface. The latter is calculated from the equation $2\kappa = \nabla\cdot\mathbf{n}$. The tangent and the normal to the free surface, which is defined as $r^* = r_0 - h^*(\theta,t)$, are given by equations:

$$\mathbf{t} = \left(-\frac{\partial h^*}{\partial\theta}\mathbf{e}_r + r^*\mathbf{e}_\theta\right)\Big/\left(\left(\frac{\partial h^*}{\partial\theta}\right)^2 + r^{*2}\right)^{1/2} \quad \text{and} \quad \mathbf{n} = -\left(\mathbf{e}_r + \frac{1}{r^*}\frac{\partial h^*}{\partial\theta}\mathbf{e}_\theta\right)\Big/\left(1+\left(\frac{1}{r^*}\frac{\partial h^*}{\partial\theta}\right)^2\right)^{1/2}.$$

On the wall of the cylinder, where $r^* = r_0$, the no-slip condition, $\mathbf{v}^* = (v^*_r, v^*_\theta) = (0, \Omega r_0)$, is satisfied. Reynolds number is negligibly small, such that in the Navier-Stokes equations, the inertial forces can be ignored. The Navier-Stokes and Oldroyd-B constitutive equations in cylindrical coordinates are given in [21]:

$$\frac{1}{r^*}\frac{\partial}{\partial r^*}\left(r^* v^*_r\right) + \frac{1}{r^*}\frac{\partial v^*_\theta}{\partial\theta} = 0 \tag{5}$$

$$-\rho g\sin\theta - \frac{\partial p^*}{\partial r^*} + \frac{\partial\tau^*_{rr}}{\partial r^*} + \left(\frac{\tau^*_{rr}-\tau^*_{\theta\theta}}{r^*}\right) + \frac{1}{r^*}\frac{\partial\tau^*_{\theta r}}{\partial\theta} = 0 \tag{6}$$

$$-\rho g\cos\theta - \frac{1}{r^*}\frac{\partial p^*}{\partial\theta} + \frac{1}{r^*}\frac{\partial\tau^*_{\theta\theta}}{\partial\theta} + \frac{\partial\tau^*_{r\theta}}{\partial r^*} + \frac{2}{r^*}\tau^*_{r\theta} = 0 \tag{7}$$

$$\begin{aligned}
&\tau^*_{r\theta} + \lambda_1\left[\frac{\partial\tau^*_{r\theta}}{\partial t^*} + v^*_r\frac{\partial\tau^*_{r\theta}}{\partial r^*} + \frac{v^*_\theta}{r^*}\frac{\partial\tau^*_{r\theta}}{\partial\theta} - 2\frac{v^*_\theta}{r^*}\left(\tau^*_{rr}-\tau^*_{\theta\theta}\right) - \left(\frac{\partial v^*_r}{\partial r^*}\tau^*_{r\theta} + \left(\frac{1}{r^*}\frac{\partial v^*_r}{\partial\theta} - \frac{v^*_\theta}{r^*}\right)\tau^*_{\theta\theta}\right)\right.\\
&\left. - \left(\frac{\partial v^*_\theta}{\partial r^*}\tau^*_{rr} + \left(\frac{1}{r^*}\frac{\partial v^*_\theta}{\partial\theta} + \frac{v^*_r}{r^*}\right)\tau^*_{\theta r}\right)\right] = 2\mu\left[D^*_{r\theta} + \lambda_2\left[\frac{\partial D^*_{r\theta}}{\partial t^*} + v^*_r\frac{\partial D^*_{r\theta}}{\partial r^*} + \frac{v^*_\theta}{r^*}\frac{\partial D^*_{r\theta}}{\partial\theta}\right.\right.\\
&\left.\left. + \frac{v^*_\theta}{r^*}\left(D^*_{rr} - D^*_{\theta\theta}\right) - \left(\frac{\partial v^*_r}{\partial r^*}D^*_{r\theta} + \left(\frac{1}{r^*}\frac{\partial v^*_r}{\partial\theta} - \frac{v^*_\theta}{r^*}\right)D^*_{\theta\theta}\right) - \left(\frac{\partial v^*_\theta}{\partial r^*}D^*_{rr} + \left(\frac{1}{r^*}\frac{\partial v^*_\theta}{\partial\theta} + \frac{v^*_r}{r^*}\right)D^*_{\theta r}\right)\right]
\end{aligned} \tag{8}$$

$$\begin{aligned}
&\tau^*_{rr} + \lambda_1\left[\frac{\partial\tau^*_{rr}}{\partial t^*} + v^*_r\frac{\partial\tau^*_{rr}}{\partial r^*} + \frac{v^*_\theta}{r^*}\frac{\partial\tau^*_{rr}}{\partial\theta} - 2\frac{v^*_\theta}{r^*}\tau^*_{r\theta} - 2\left(\frac{\partial v^*_r}{\partial r^*}\tau^*_{rr} + \left(\frac{1}{r^*}\frac{\partial v^*_r}{\partial\theta} - \frac{v^*_\theta}{r^*}\right)\tau^*_{\theta r}\right)\right] =\\
&2\mu\left[D^*_{rr} + \lambda_2\left[\frac{\partial D^*_{rr}}{\partial t^*} + v^*_r\frac{\partial D^*_{rr}}{\partial r^*} + \frac{v^*_\theta}{r^*}\frac{\partial D^*_{rr}}{\partial\theta} - 2\frac{v^*_\theta}{r^*}D^*_{r\theta} - 2\left(\frac{\partial v^*_r}{\partial r^*}D^*_{rr} + \left(\frac{1}{r^*}\frac{\partial v^*_r}{\partial\theta} - \frac{v^*_\theta}{r^*}\right)D^*_{\theta r}\right)\right]\right]
\end{aligned} \tag{9}$$

$$\tau^*_{\theta\theta}+\lambda_1\left[\frac{\partial\tau^*_{\theta\theta}}{\partial t^*}+v^*_r\frac{\partial\tau^*_{\theta\theta}}{\partial r^*}+\frac{v^*_\theta}{r^*}\frac{\partial\tau^*_{\theta\theta}}{\partial\theta}+2\frac{v^*_\theta}{r^*}\tau^*_{r\theta}-2\left(\frac{\partial v^*_\theta}{\partial r^*}\tau^*_{r\theta}+\left(\frac{1}{r^*}\frac{\partial v^*_\theta}{\partial\theta}+\frac{v^*_r}{r^*}\right)\tau^*_{\theta\theta}\right)\right]$$
$$=2\mu\left[D^*_{\theta\theta}+\lambda_2\left[\frac{\partial D^*_{\theta\theta}}{\partial t^*}+v^*_r\frac{\partial D^*_{\theta\theta}}{\partial r^*}+\frac{v^*_\theta}{r^*}\frac{\partial D^*_{\theta\theta}}{\partial\theta}+2\frac{v^*_\theta}{r^*}D^*_{r\theta}\right.\right. \tag{10}$$
$$\left.\left.-2\left(\frac{\partial v^*_\theta}{\partial r^*}D^*_{r\theta}+\left(\frac{1}{r^*}\frac{\partial v^*_\theta}{\partial\theta}+\frac{v^*_r}{r^*}\right)D^*_{\theta\theta}\right)\right]\right]$$

The scaling of position, pressure, velocity, and shear stress components in rimming flow is well documented [14]:

$$r^* \sim r_0,\ h^* \sim h_0,\ p^* \sim g\rho r_0,\ v^*_\theta \sim \Omega r_0,\ v^*_r \sim \Omega r_0\delta\ \ \tau^*_{r\theta} \sim \mu\Omega/\delta,$$
$$t^* \sim 1/\Omega^*,\ D^*_{\theta\theta} \sim \Omega^*,\ D^*_{r\theta} \sim \Omega^*/\delta,\ D^*_{rr} \sim -\Omega^*, \tag{11}$$

where δ is the ratio of the unknown characteristic thickness to the radius of the cylinder, $\delta = h_0/r_0$. Scales for normal stresses are determined by ensuring the term balance in the constitutive equation (3). As was shown in [22], a solution to a similar problem of a thin Oldroyd-B film along an axisymmetric substrate, the scale for the azimuthal normal stress $\tau^*_{\theta\theta}$ should be set as $\mu\Omega/\delta^2$. In this case, while $\tau^*_{\theta\theta}$ does not depend strongly on the rate of azimuthal elongation, as is the case for shear dominated thin-film flow, it does not vanish because of the non-linear coupling with shear effects present in the upper-convective terms in equation (3). Similarly, the scale of the radial stress, τ^*_{rr}, should be taken as $\mu\Omega$, which ensures the survival of all terms in equation (3) that govern τ^*_{rr} and $\tau^*_{r\theta}$. So, introducing the following non-dimensional variables,

$$v_\theta = \frac{v^*_\theta}{\Omega\ r_0},\qquad v_R = \frac{v^*_r}{\delta\Omega\ r_0},\qquad R = \frac{1}{\delta}-\frac{r^*}{\delta r_0},\qquad p = \frac{p^*}{\rho\ g\ r_0}$$
$$\tau_{RR} = \frac{\tau^*_{rr}}{\mu\ \Omega},\qquad \tau_{R\theta} = \frac{\delta\,\tau^*_{R\theta}}{\mu\ \Omega},\qquad \tau_{\theta\theta} = \frac{\delta^2\tau^*_{\theta\theta}}{\mu\ \Omega},\qquad D_{\theta\theta} = \frac{D^*_{\theta\theta}}{\Omega}, \tag{12}$$
$$D_{R\theta} = \frac{\delta\,D^*_{R\theta}}{\Omega}\qquad D_{RR} = -\frac{D^*_{rr}}{\Omega}\qquad t = \frac{t^*}{\Omega}$$

the governing equations can be presented in the non-dimensional form:

$$\frac{-\partial\left(\left(1-\delta R\right)v_R\right)}{\partial R}+\frac{\partial v_\theta}{\partial\theta}=0 \tag{13}$$

$$-\delta\sin\theta-\frac{\partial p}{\partial R}-\delta^2\frac{\partial\tau_{RR}}{\partial R}+\frac{\delta^3\tau_{RR}}{\left(1-\delta R\right)}-\frac{\delta\tau_{\theta\theta}}{\left(1-\delta R\right)}+\frac{\delta^2}{\left(1-\delta R\right)}\frac{\partial\tau_{R\theta}}{\partial\theta}=0 \tag{14}$$

$$-\cos\theta-\frac{1}{(1-\delta R)}\frac{\partial p}{\partial\theta}+\frac{1}{(1-\delta R)}\frac{\partial\tau_{\theta\theta}}{\partial\theta}-\frac{\partial\tau_{R\theta}}{\partial R}+\frac{2\delta\tau_{R\theta}}{(1-\delta R)}=0 \tag{15}$$

$$\begin{aligned}&\tau_{RR}+De\left[\frac{\partial\tau_{RR}}{\partial t}-v_R\frac{\partial\tau_{RR}}{\partial R}+\frac{v_\theta}{(1-\delta R)}\frac{\partial\tau_{RR}}{\partial\theta}-2\frac{v_\theta\tau_{R\theta}}{\delta(1-\delta R)}+2\tau_{RR}\frac{\partial v_R}{\partial R}-2\frac{\tau_{R\theta}}{(1-\delta R)}\frac{\partial v_R}{\partial\theta}\right.\\&\left.+2\frac{\tau_{R\theta}}{\delta(1-\delta R)}v_\theta\right]=2\mu\left[\mathrm{D}_{RR}+De\cdot K\left[\frac{\partial D_{RR}}{\partial t}-v_R\frac{\partial D_{RR}}{\partial R}+\frac{v_\theta}{(1-\delta R)}\frac{\partial D_{RR}}{\partial\theta}-2\frac{v_\theta\tau_{R\theta}}{\delta(1-\delta R)}+2\mathrm{D}_{RR}\frac{\partial v_R}{\partial R}\right.\right.\\&\left.\left.-2\frac{D_{R\theta}}{(1-\delta R)}\frac{\partial v_R}{\partial\theta}+2\frac{D_{R\theta}}{\delta(1-\delta R)}v_\theta\right]\right]\end{aligned} \tag{16}$$

$$\begin{aligned}&\tau_{R\theta}+De\left[\frac{\partial\tau_{R\theta}}{\partial t}-v_R\frac{\partial\tau_{R\theta}}{\partial R}+\frac{v_\theta}{1-\delta R}\frac{\partial\tau_{R\theta}}{\partial\theta}+\frac{\delta v_\theta\tau_{RR}}{1-\delta R}+\tau_{R\theta}\frac{\partial v_R}{\partial R}-\frac{\tau_{\theta\theta}}{1-\delta R}\frac{\partial v_R}{\partial\theta}\right.\\&\left.+\tau_{RR}\frac{\partial v_\theta}{\partial R}-\frac{\tau_{R\theta}}{1-\delta R}\frac{\partial v_\theta}{\partial\theta}-\frac{\delta v_R\tau_{\theta R}}{1-\delta R}\right]\\&=2\mu\left[D_{R\theta}+De\cdot K\left(\frac{\partial D_{R\theta}}{\partial t}+-v_R\frac{\partial}{\partial R}D_{R\theta}+\frac{v_\theta}{R}\frac{\partial}{\partial\theta}D_{R\theta}+\right)\frac{v_\theta\delta}{R}\left(D_{RR}-D_{\theta\theta}\right)\right.\\&\left.-\frac{\partial v_R}{\partial R}D_{R\theta}-\frac{1}{1-\delta R}D_{\theta\theta}\left(\delta^2\frac{\partial v_R}{\partial\theta}-\delta v_\theta\right)-\frac{\delta\partial v_\theta}{\partial R}D_{RR}-\frac{1}{1-\delta R}D_{R\theta}\left(\frac{\partial v_\theta}{\partial\theta}+v_R\right)\right)\right]\end{aligned} \tag{17}$$

$$\begin{aligned}&\tau_{\theta\theta}+De\left[\frac{\partial\tau_{\theta\theta}}{\partial t}-v_R\frac{\partial\tau_{\theta\theta}}{\partial R}+\frac{v_\theta}{1-\delta R}\frac{\partial\tau_{\theta\theta}}{\partial\theta}+\frac{2\delta}{(1-\delta R)}\tau_{R\theta}v_\theta+2\tau_{R\theta}\frac{\partial v_\theta}{\partial R}-\frac{2}{1-\delta R}\tau_{\theta\theta}\frac{\partial v_\theta}{\partial\theta}\right.\\&\left.-\frac{2\delta}{1-\delta R}\tau_{\theta\theta}v_R\right]=2\mu\left[D_{\theta\theta}+DeK\left[\frac{\partial D_{\theta\theta}}{\partial t}-v_R\frac{\partial D_{\theta\theta}}{\partial R}+\frac{v_\theta}{1-\delta R}\frac{\partial D_{\theta\theta}}{\partial\theta}+\frac{2\delta}{(1-\delta R)}D_{R\theta}v_\theta+2D_{R\theta}\frac{\partial v_\theta}{\partial R}\right.\right.\\&\left.\left.-\frac{2}{1-\delta R}D_{\theta\theta}\frac{\partial v_\theta}{\partial\theta}-\frac{2\delta}{1-\delta R}D_{\theta\theta}v_R\right]\right.\end{aligned} \tag{18}$$

In the above equations, parameter $\delta=\left(\frac{\mu_0\Omega}{\rho g r_0}\right)^{1/2}$ is obtained as a result of scale analysis [3] equating the viscous and gravitational forces in equation (15). It is worth noting that for major applications, e.g. for rotational molding, the value of δ is in the range of 10^{-3} to 10^{-1} [13]. Exploiting the fact that δ is very small and, to this end, ignoring the terms of $O(\delta)$, the non-dimensional governing equations in cylindrical coordinates reduce to

$$-\frac{\partial v_R}{\partial R}+\frac{\partial v_\theta}{\partial\theta}=0 \tag{19}$$

$$\frac{\partial p}{\partial R}=0 \tag{20}$$

$$-\cos\theta-\frac{\partial p}{\partial\theta}+\frac{\partial\tau_{\theta\theta}}{\partial\theta}-\frac{\partial\tau_{R\theta}}{\partial R}=0 \tag{21}$$

$$\tau_{R\theta}+De\left[\frac{\partial\tau_{R\theta}}{\partial t}-v_R\frac{\partial\tau_{R\theta}}{\partial R}+v_\theta\frac{\partial\tau_{R\theta}}{\partial\theta}-\tau_{\theta\theta}\frac{\partial v_R}{\partial\theta}+\tau_{RR}\frac{\partial v_\theta}{\partial R}+\tau_{R\theta}\frac{\partial v_R}{\partial R}-\tau_{R\theta}\frac{\partial v_\theta}{\partial\theta}\right]+\frac{\partial v_\theta}{\partial R}$$
$$-De\cdot K\left[\frac{\partial D_{R\theta}}{\partial t}+v_R\frac{\partial^2 v_\theta}{\partial R^2}-v_\theta\frac{\partial^2 v_\theta}{\partial\theta\partial R}-3\frac{\partial v_R}{\partial R}\frac{\partial v_\theta}{\partial R}+\frac{\partial v_\theta}{\partial R}\frac{\partial v_\theta}{\partial\theta}\right]=0 \quad (22)$$

$$\tau_{RR}+De\left[\frac{\partial\tau_{RR}}{\partial t}-v_R\frac{\partial\tau_{RR}}{\partial R}+v_\theta\frac{\partial\tau_{RR}}{\partial\theta}+2\tau_{RR}\frac{\partial v_R}{\partial R}-2\tau_{R\theta}\frac{\partial v_R}{\partial\theta}\right]-2\left[\frac{\partial D_{RR}}{\partial t}-\frac{\partial v_R}{\partial R}+\right.$$
$$\left.De\cdot K\left[v_R\frac{\partial^2 v_R}{\partial R^2}-v_\theta\frac{\partial^2 v_R}{\partial\theta\partial R}-2\left(\frac{\partial v_R}{\partial R}\right)^2+\frac{\partial v_R}{\partial\theta}\frac{\partial v_\theta}{\partial R}\right]\right]=0 \quad (23)$$

$$\tau_{\theta\theta}+De\left[\frac{\partial\tau_{\theta\theta}}{\partial t}-v_R\frac{\partial\tau_{\theta\theta}}{\partial R}+v_\theta\frac{\partial\tau_{\theta\theta}}{\partial\theta}+2\frac{\partial v_\theta}{\partial R}\tau_{R\theta}-2\tau_{\theta\theta}\frac{\partial v_\theta}{\partial\theta}\right]+2De\cdot\left[\frac{\partial D_{\theta\theta}}{\partial t}+\left(\frac{\partial v_\theta}{\partial R}\right)^2\right]=0 \quad (24)$$

Scale analysis of the boundary conditions on the free surface (4) gives a new non-dimensional parameter $C_B=\delta^2\dfrac{\sigma}{r_0\,\mu_0\Omega}$. This parameter is the inverse of the Bond number, which characterizes the ratio of capillary forces to gravitational forces. Since C_B <<1 for rimming flow and, therefore, the surface tension effects can be neglected, the boundary conditions on the free surface (4) in non-dimensional form yield:

$$-p+\delta^2\tau_{RR}+\frac{2\delta^2\tau_{R\theta}}{1-\delta R}\frac{\partial h}{\partial\theta}+\frac{\delta^2}{(1-\delta R)^2}\left(\frac{\partial h}{\partial\theta}\right)^2\tau_{\theta\theta}=0 \quad (25)$$

$$-\frac{\delta^2\tau_{RR}}{1-\delta R}\frac{\partial h}{\partial\theta}-\frac{\delta^2\tau_{R\theta}}{(1-\delta R)^2}\left(\frac{\partial h}{\partial\theta}\right)^2+\tau_{R\theta}+\frac{\tau_{\theta\theta}}{1-\delta R}\frac{\partial h}{\partial\theta}=0 \quad (26)$$

Dropping terms of $O(\delta)$ reduces equations (25) and (26), at $R = h$, to:

$$p=0 \quad (27)$$

$$\tau_{R\theta}+\tau_{\theta\theta}\frac{\partial h}{\partial\theta}=0 \quad (28)$$

The non-dimensional boundary conditions on the wall of the cylinder, $R = 0$, are:

$$v_\theta=1,\ v_R=0 \quad (29)$$

From equation (20), pressure is constant in the radial direction. So, with boundary condition (27), we find $p = 0$ everywhere in the film. Therefore, equation (21) reduces to:

$$-\cos\theta+\frac{\partial\tau_{\theta\theta}}{\partial\theta}-\frac{\partial\tau_{R\theta}}{\partial R}=0 \quad (30)$$

3. Asymptotic Model

Unfortunately, even in this simplified form, the boundary value problem (19), (22)-(24), (27)-(30) can be solved only numerically. However, as it was pointed out by Lawrence and Zhou [19] and Jenekhe & Schuldt [20], for many polymeric solutions, the characteristic time of relaxation, λ_1, which characterizes memory effects, is small and in many cases stays in the range of 10^{-2} s- 10^{-1}s. The time scale for rimming flow associated with rotation is T=1/Ω. Hence, the Deborah number, $De = \lambda_1 / T$, for the typical rotational rates, Ω, that occur in rotational molding (~10 rad s^{-1}) is in many cases below 1 (De < 1). Due to the presence of the small parameter De, the simplified model, (19), (22)-(24), and (27)-(30) can be solved by implementing an asymptotic expansion.

To perform the expansion of the unknowns, the following change of variables is introduced:

$$x = \theta, y = \frac{R}{h(\theta)}, t = t \tag{31}$$

As a result, the initial domain for R, $[0, h(\theta,t)]$, with moving boundary $h(\theta,t)$, is converted to a domain with fixed boundaries for y, [0,1]. Since in new variables (31) the derivatives can be readily calculated using the chain rule as $\frac{\partial f}{\partial \theta} = \frac{\partial f}{\partial x} - \frac{y}{h}\frac{\partial h}{\partial x}\frac{\partial f}{\partial y}, \frac{df}{\partial R} = \frac{1}{h}\frac{\partial f}{\partial y}, \frac{\partial f}{\partial t} = \frac{\partial f}{\partial t} - \frac{y}{h}\frac{\partial h}{\partial t}\frac{\partial f}{\partial y}$, the governing equations take the following form:

$$-\frac{1}{h}\frac{\partial v_R}{\partial y} + \frac{\partial v_\theta}{\partial x} - \frac{y}{h}\frac{\partial h}{\partial x}\frac{\partial v_\theta}{\partial y} = 0 \tag{32}$$

$$\frac{\partial p}{\partial y} = 0 \tag{33}$$

$$-\cos\theta + \frac{\partial \tau_{\theta\theta}}{\partial x} - \frac{y}{h}\frac{\partial h}{\partial x}\frac{\partial \tau_{\theta\theta}}{\partial y} - \frac{1}{h}\frac{\partial \tau_{R\theta}}{\partial y} = 0 \tag{34}$$

$$\tau_{RR} + De\left[\frac{\partial \tau_{RR}}{\partial t} - v_R\left(\frac{1}{h}\frac{\partial \tau_{RR}}{\partial y}\right) + v_\theta\left(\frac{\partial \tau_{RR}}{\partial x} - \frac{y}{h}\frac{\partial h}{\partial x}\frac{\partial \tau_{RR}}{\partial y}\right) + 2\tau_{RR}\frac{1}{h}\frac{\partial v_R}{\partial y} - 2\tau_{R\theta}\left(\frac{\partial v_R}{\partial x}\right.\right.$$
$$\left.\left. - \frac{y}{h}\frac{\partial h}{\partial x}\frac{\partial v_R}{\partial y}\right)\right] - 2\left[-\frac{1}{h}\frac{\partial v_R}{\partial y} + De\cdot K\left[\frac{\partial D_{RR}}{\partial t} + v_R\frac{1}{h^2}\frac{\partial^2 v_R}{\partial y^2} - v_\theta\frac{1}{h}\frac{\partial}{\partial y}\left(\frac{\partial v_R}{\partial x} - \frac{y}{h}\frac{\partial h}{\partial x}\frac{\partial v_R}{\partial y}\right) - 2\left(\frac{1}{h}\frac{\partial v_R}{\partial y}\right)^2\right.\right.$$
$$\left.\left. + \left(\frac{\partial v_R}{\partial x} - \frac{y}{h}\frac{\partial h}{\partial x}\frac{\partial v_R}{\partial y}\right)\frac{1}{h}\frac{\partial v_\theta}{\partial y}\right]\right] = 0 \tag{35}$$

$$\tau_{R\theta} + De\left[\frac{\partial \tau_{R\theta}}{\partial t} - v_R \frac{1}{h}\frac{\partial \tau_{R\theta}}{\partial y} + v_\theta\left(\frac{\partial \tau_{R\theta}}{\partial x} - \frac{y}{h}\frac{\partial h}{\partial x}\frac{\partial \tau_{R\theta}}{\partial y}\right) - \tau_{\theta\theta}\left(\frac{\partial v_R}{\partial x} - \frac{y}{h}\frac{\partial h}{\partial x}\frac{\partial v_R}{\partial y}\right) + \tau_{RR}\frac{1}{h}\frac{\partial v_\theta}{\partial y} + \tau_{R\theta}\frac{1}{h}\frac{\partial v_R}{\partial y}\right.$$
$$\left. - \tau_{R\theta}\left(\frac{\partial v_\theta}{\partial x} - \frac{y}{h}\frac{\partial h}{\partial x}\frac{\partial v_\theta}{\partial y}\right)\right] + \frac{1}{h}\frac{\partial v_\theta}{\partial y} - De\cdot K\left[\frac{\partial D_{R\theta}}{\partial t} + v_R\frac{1}{h^2}\frac{\partial^2 v_\theta}{\partial y^2} - v_\theta\frac{1}{h}\frac{\partial}{\partial y}\left(\frac{\partial v_\theta}{\partial x} - \frac{y}{h}\frac{\partial h}{\partial x}\frac{\partial v_\theta}{\partial y}\right)\right. \quad (36)$$
$$\left. - 3\frac{1}{h^2}\frac{\partial v_R}{\partial y}\frac{\partial v_\theta}{\partial y} + \frac{1}{h}\left(\frac{\partial v_\theta}{\partial x} - \frac{y}{h}\frac{\partial h}{\partial x}\frac{\partial v_\theta}{\partial y}\right)\frac{\partial v_\theta}{\partial y}\right] = 0$$

$$\tau_{\theta\theta} + De\left[\frac{\partial \tau_{\theta\theta}}{\partial t} - \frac{1}{h}v_R\frac{\partial \tau_{\theta\theta}}{\partial y} + v_\theta\left(\frac{\partial \tau_{\theta\theta}}{\partial x} - \frac{y}{h}\frac{\partial h}{\partial x}\frac{\partial \tau_{\theta\theta}}{\partial y}\right) + 2\frac{1}{h}\frac{\partial v_\theta}{\partial y}\tau_{\bar{R}\theta} - 2\tau_{\theta\theta}\left(\frac{\partial v_\theta}{\partial x} - \frac{y}{h}\frac{\partial h}{\partial x}\frac{\partial v_\theta}{\partial y}\right)\right] \quad (37)$$
$$+ 2De\cdot K\left[\frac{\partial \tau_{\theta\theta}}{\partial t} + \left(\frac{1}{h}\frac{\partial v_\theta}{\partial y}\right)^2\right] = 0$$

Boundary conditions (28) and (29) are now respectively implemented for $y = 1$ and $y = 0$.

Equations (28), (29), and (32)-(37) can now be expanded. As shown in [23], asymptotic series can diverge even with small parameters. A rule of thumb can usually be implemented to optimally truncate the series. In this case, the optimal order of truncation of accuracy $O(De^{N+1})$ is:

$$N \sim 1/De - 1 \quad (38)$$

For example, if $De = ½$, the series can be truncated to the first order of $N = 1$ with accuracy of $O(De^2)$. If N is taken to be larger, error tends to accumulate, and as $N\to\infty$, the error associated with this lack of truncation can grow without bounds. Orders of truncation and expansion are therefore dependent on the size of De. While higher order approximations may be more accurate, their scope is more limited to very weakly viscoelastic fluids, since De must decrease for larger N.

A first order, $N = 1$, approximation can be used to model weakly viscoelastic fluids with acceptable accuracy and flexibility.

The following first order asymptotic expansions are implemented for $De \le ½$:

$$\begin{aligned}
v_\theta &= v_\theta^{<0>} + De\cdot v_\theta^{<1>} + O(De^2)\\
v_R &= v_R^{<0>} + De\cdot v_R^{<1>} + O(De^2)\\
\tau_{RR} &= \tau_{RR}^{<0>} + De\cdot \tau_{RR}^{<1>} + O(De^2)\\
\tau_{R\theta} &= \tau_{R\theta}^{<0>} + De\cdot \tau_{R\theta}^{<1>} + O(De^2)\\
\tau_{\theta\theta} &= \tau_{\theta\theta}^{<0>} + De\cdot \tau_{\theta\theta}^{<1>} + O(De^2)\\
h &= h_0 + De\cdot h_1 + O(De^2)
\end{aligned} \quad (39)$$

The above formulae are substituted into the governing equations (32)-(37) and boundary conditions (29)-(30). Collecting terms of the same order of De yields leading order and first order systems of equations.

The leading order asymptotic system is given by terms of $O(1)$:

$$\frac{-\partial v_R^{<0>}}{\partial R} - y\cdot\frac{dh_0}{dx}\frac{\partial v_\theta^{<0>}}{\partial x} + h_0\frac{\partial v_\theta^{<0>}}{\partial y} = 0 \quad (40)$$

$$h_0 \cdot \cos\theta + \frac{\partial \tau_{R\theta}^{<0>}}{\partial y} - y \cdot \frac{dh_0}{dx} \frac{\partial \tau_{\theta\theta}^{<0>}}{\partial y} + h_0 \frac{\partial \tau_{\theta\theta}^{<0>}}{\partial y} = 0 \tag{41}$$

$$h_0{}^2 \tau_{RR}^{<0>} + 2h_0 \frac{\partial v_R^{<0>}}{\partial y} = 0 \tag{42}$$

$$h_0{}^2 \tau_{R\theta}^{<0>} + h_0 \frac{\partial v_\theta^{<0>}}{\partial y} = 0 \tag{43}$$

$$h_0{}^2 \tau_{\theta\theta}^{<0>} = 0 \tag{44}$$

The corresponding boundary conditions on the wall of the cylinder and free surface are respectively:

$$y=0, \quad v_\theta^{<0>} = 1, \quad v_R^{<0>} = 0, \tag{45}$$

$$y=1, \quad \tau_{R\theta}^{<0>} + \tau_{\theta\theta}^{<0>} \frac{\partial h_0}{\partial x} = 0. \tag{46}$$

The first order asymptotic system is given by terms of $O(De)$:

$$-\frac{\partial v_R^{<1>}}{\partial y} - y \cdot \frac{dh_1}{dx} \frac{\partial v_\theta^{<1>}}{\partial y} + h_1 \frac{\partial v_\theta^{<0>}}{\partial x} + h_0 \frac{\partial v_\theta^{<1>}}{\partial x} = 0 \tag{47}$$

$$-h_1 \cos(x) - \frac{\partial \tau_{R\theta}^{<1>}}{\partial y} - \frac{\partial \tau_{\theta\theta}^{<1>}}{\partial y} - y \cdot \frac{dh_1}{dx} \frac{\partial \tau_{\theta\theta}^{<0>}}{\partial y} - y \frac{dh_0}{dx} \frac{\partial \tau_{\theta\theta}^{<1>}}{\partial y} + h_1 \frac{\partial \tau_{\theta\theta}^{<1>}}{\partial x} + h_0 \frac{\partial \tau_{\theta\theta}^{<1>}}{\partial x} = 0 \tag{48}$$

$$\begin{aligned}
&h_0^2 \frac{\partial \tau_{RR}^{<0>}}{\partial t} + h_0^2 \tau_{RR}^{<1>} + 2h_1 h_0 \tau_{RR}^{<0>} - h_0 v_R^{<0>} \frac{\partial \tau_{RR}^{<0>}}{\partial y} - y h_0 . v_\theta^{<0>} \frac{dh_0}{dx} \frac{\partial \tau_{RR}^{<0>}}{\partial y} + 2h_1 \frac{\partial v_R^{<0>}}{\partial y} \\
&+ 2h_0 \tau_{RR}^{<0>} \frac{\partial v_R^{<0>}}{\partial y} + 2y h_0 \frac{dh_0}{dx} \tau_{R\theta}^{<0>} \frac{\partial v_R^{<0>}}{\partial y} - 2K \cdot \frac{dh_0}{dx} v_\theta^{<0>} \frac{\partial v_R^{<0>}}{\partial y} + 4K \left(\frac{\partial v_R^{<0>}}{\partial y} \right)^2 \\
&+ 2h_0 \frac{\partial v_R^{<1>}}{\partial y} + 2Kh_0 \frac{\partial v_R^{<0>}}{\partial y \partial t} + 2K \cdot y \frac{dh}{dx} \frac{\partial v_R^{<0>}}{\partial y} \frac{\partial v_\theta^{<0>}}{\partial y} - 2K \cdot v_R^{<0>} \frac{\partial^2 v_R^{<0>}}{\partial y^2} \\
&- 2K \cdot y \cdot \frac{dh_0}{dx} v_\theta^{<0>} \frac{\partial^2 v_R^{<0>}}{\partial y^2} + h_0^2 \cdot v_\theta^{<0>} \frac{\partial \tau_{RR}^{<0>}}{\partial x} - 2h_0^2 \tau_{R\theta}^{<0>} \frac{\partial v_R^{<0>}}{\partial x} \\
&- 2K \cdot h_0 \frac{\partial v_\theta^{<0>}}{\partial y} \frac{\partial v_R^{<0>}}{\partial x} + 2K \cdot h_0 \cdot v_\theta^{<0>} \frac{\partial^2 v_R^{<0>}}{\partial x \partial y} = 0
\end{aligned} \tag{49}$$

$$h_0^2\frac{\partial\tau_{R\theta}^{<0>}}{\partial t}+h_0^2\tau_{R\theta}^{<1>}+2h_1h_0\tau_{R\theta}^{<0>}-h_0v_R^{<0>}\frac{\partial\tau_{R\theta}^{<0>}}{\partial y}-yh_0v_\theta^{<0>}\frac{dh_0}{dx}\frac{\partial\tau_{R\theta}^{<0>}}{\partial y}+h_0\tau_{R\theta}^{<0>}\frac{\partial v_R^{<0>}}{\partial y}$$
$$+yh_0\frac{dh_0}{dx}\frac{\partial v_R^{<0>}}{\partial y}\tau_{\theta\theta}^{<0>}+h_1\frac{\partial v_\theta^{<0>}}{\partial y}+h_0\tau_{RR}^{<0>}\frac{\partial v_\theta^{<0>}}{\partial y}+yh_0\frac{dh_0}{dx}\frac{\partial v_\theta^{<0>}}{\partial y}\tau_{R\theta}^{<0>}+h_0^2v_\theta^{<0>}\frac{\partial\tau_{R\theta}^{<0>}}{\partial x}$$
$$-h_0^2\frac{\partial v_R^{<0>}}{\partial x}\tau_{\theta\theta}^{<0>}-h_0^2\frac{\partial v_\theta^{<0>}}{\partial x}\tau_{R\theta}^{<0>}+h_0\frac{\partial v_\theta^{<1>}}{\partial y}-Kv_\theta^{<0>}\frac{dh_0}{dx}\frac{\partial v_\theta^{<0>}}{\partial y}+3K\frac{\partial v_R^{<0>}}{\partial y}\frac{\partial v_\theta^{<0>}}{\partial y} \tag{50}$$
$$+Kh_0\frac{\partial^2 v_\theta^{<0>}}{\partial y\partial t}+K\cdot y\frac{dh_0}{dx}\left(\frac{\partial v_\theta^{<0>}}{\partial y}\right)^2-Kv_R^{<0>}\frac{\partial^2 v_\theta^{<0>}}{\partial y^2}-Kv_\theta^{<0>}y\frac{dh_0}{dx}\frac{\partial^2 v_\theta^{<0>}}{\partial y^2}$$
$$-K\cdot h_0\frac{\partial v_\theta^{<0>}}{\partial y}\frac{\partial v_\theta^{<0>}}{\partial x}+K\cdot h_0v_\theta^{<0>}\frac{\partial^2 v_\theta^{<0>}}{\partial x\partial y}=0$$

$$h_0^2\frac{\partial\tau_{\theta\theta}^{<0>}}{\partial t}+h_0^2\tau_{\theta\theta}^{<1>}+2h_1h_0\tau_{\theta\theta}^{<0>}-h_0v_R^{<0>}\frac{\partial\tau_{\theta\theta}^{<0>}}{\partial y}-yh_0v_\theta^{<0>}\frac{dh_0}{dx}\frac{\partial\tau_{\theta\theta}^{<0>}}{\partial y}$$
$$+2h_0\tau_{R\theta}^{<0>}\frac{\partial v_\theta^{<0>}}{\partial y}+2yh_0\tau_{\theta\theta}^{<0>}\frac{dh_0}{dx}\frac{\partial v_\theta^{<0>}}{\partial y}-2h_0^2\tau_{\theta\theta}^{<0>}\frac{\partial v_\theta^{<0>}}{\partial x}+2K\left(\frac{\partial v_\theta^{<0>}}{\partial y}\right)^2=0 \tag{51}$$

The corresponding boundary conditions at the wall of the cylinder and free surface are:

$$y=0,\qquad v_\theta^{<1>}=0,\qquad v_R^{<1>}=0, \tag{52}$$

and

$$y=1,\qquad \tau_{R\theta}^{<1>}+\frac{\partial h_0}{\partial x}\tau_{\theta\theta}^{<1>}+\frac{\partial h_1}{\partial x}\tau_{\theta\theta}^{<0>}=0. \tag{53}$$

Solutions to the leading order (40)-(44) and 1st order (47)-(51) systems are presented below. Equation (44) reduces to $\tau_{\theta\theta}^{<0>}=0$ and (41) can be integrated. Accounting for boundary condition (46),

$$\tau_{R\theta}^{<0>}=h_0\cos(x)-y\cdot h_0\cos(x) \tag{54}$$

Accounting for solution (54) and boundary condition (45), $v_\theta^{<0>}$, the azimuthal velocity, can be found by integrating equation (43) with respect to *y*,

$$v_\theta^{<0>}=\frac{1}{2}y^2h_0^2\cos(x)-yh_0^2\cos(x)+1 \tag{55}$$

The radial component of velocity, $v_R^{<0>}$, can be found using equations (40) and (55) with boundary condition (45):

$$v_R^{<0>}=-\frac{1}{2}y^2\frac{dh_0}{dx}h_0^2\cos(x)-\frac{1}{6}y^3h_0^3\sin(x)+\frac{1}{2}y^2h_0^3\sin(x) \tag{56}$$

Accounting for equation (56), the normal stress, $\tau_{RR}^{<0>}$, from equation (42), is found:

$$\tau_{RR}^{<0>}=2yh_0\frac{dh_0}{dx}\cos(x)+y^2h_0^{\,2}\sin(x)-2y\cdot h_0^{\,2}\sin(x) \tag{57}$$

Substituting the solutions (54)-(57) of the system of equations (40)-(44) into the system (47)-(51), the latter can be solved. From equation (51), it follows that

$$\tau_{\theta\theta}^{<1>} = -2(K-1)(y-1)^2\cos^2(x){h_0}^2 \tag{58}$$

Accounting for solution (58) and boundary condition (53), $\tau_{R\theta}^{<1>}$ can be found by integrating equation (48) with respect to y:

$$\tau_{R\theta}^{<1>} = \frac{1}{3}(y-1)\cos(x)\left(2(K-1)(y-1)h_0^2\left(3\cos(x)\frac{dh_0}{dx}+2(y-1)\right)h_0\sin(x)\right)-3h_1\Bigg) \tag{59}$$

The azimuthal component of velocity, $v_\theta^{<1>}$, can be obtained by integrating equation (50) with respect to *y* and accounting for boundary condition (52).

$$v_\theta^{<1>} = -\frac{1}{12}yh_0\{(K-1)[-6(y-4)\cos^2(x)\frac{\partial h_0}{\partial x}{h_0}^2-12\cos(x)\left(\frac{\partial h_0}{\partial x}+\frac{\partial h_0}{\partial t}\right) \tag{60}$$

$$+(3y-8)\sin(2x){h_0}^3-6(y-2)\sin(x)h_0]-12(y-2)\cos(x)h_1\}$$

The kinematic condition on the free surface, which represents the fact that the normal velocity of particles at the surface matches the normal velocity of the surface itself, reduces to

$$\frac{\partial h}{\partial t}+v_r+v_\theta\frac{\partial h}{\partial x}=0 \tag{61}$$

Combining equations (19) and (61) yields the partial differential equation,

$$\frac{\partial h}{\partial t}+\frac{\partial q}{\partial x}=0 \tag{62}$$

where *q*, the non-dimensional volumetric flux, is defined as

$$q=h\int_0^1 v_\theta dy \tag{63}$$

Substituting asymptotic expansions (39) into equations (62) and (63), and collecting terms of the same *O*(*De*) leads to two partial differential equations,

$$\frac{\partial h_0}{\partial t}+\frac{\partial\left[h_0\int_0^1 v_\theta^{<0>}dy\right]}{\partial x}=0 \tag{64}$$

$$\frac{\partial h_1}{\partial t}+\frac{\partial\left[\int_0^1(h_0v_\theta^{<1>}+h_1v_\theta^{<0>})dy\right]}{\partial x}=0 \tag{65}$$

4. Steady State Solutions

In the steady-state case, equation (62) reduces to:

$$\frac{\partial q}{\partial x}=0 \tag{66}$$

So, in this case q is a constant. The following algebraic equations are obtained from equation (63):

$$h_0 - \frac{1}{3}h_0^3\cos(x) = q \tag{67}$$

$$(K-1){h_0}^2[-10\cos^2(x)\frac{dh_0}{dx}{h_0}^2 + 6\cos(x)\frac{dh_0}{dx} + 3\sin(2x){h_0}^3 - 4\sin(x)h_0] \tag{68}$$
$$-12h_1(\cos(x){h_0}^2 + 1 = 0$$

As it is indicated in [24], equation (67) has three roots which can be presented in the following form:

$$h_{0,1} = \frac{2}{\sqrt{\cos(x)}}\cos\left[\frac{1}{3}\arccos\left(\frac{-3q}{2}\sqrt{\cos(x)}\right)\right] \tag{69}$$

$$h_{0,2} = \frac{2}{\sqrt{\cos(x)}}\cos\left[\frac{1}{3}\arccos\left(\frac{-3q}{2}\sqrt{\cos(x)}\right) + \frac{2\pi}{3}\right] \tag{70}$$

$$h_{0,3} = \frac{2}{\sqrt{\cos(x)}}\cos\left[\frac{1}{3}\arccos\left(\frac{-3q}{2}\sqrt{\cos(x)}\right) - \frac{2\pi}{3}\right] \tag{71}$$

Of the three roots (69)-(71), only the root (71) represents a physically meaningful solution. The root $h_{0,2}$ is negative over the whole interval, and $h_{0,1}$ is unbounded at $\theta = \pm\pi/2$ and complex outside of this interval. Whereas $h_{0,3}$ is continuous, real, and bounded over the whole interval, so expression (71) is used as h_0. The expression for h_1 is obtained in terms of h_0 by solving equation (68):

$$h_1 = \frac{(K-1)h_0^2\left[-10h_0^2\frac{dh_0}{dx}\cos^2(x) + 6\frac{dh_0}{dx}\cos(x) + 3h_0^3\sin(2x) - 4h_0\sin(x)\right]}{12(h_0^2\cos(x) - 1)} \tag{72}$$

5. Numerical Analysis of Steady State Behavior

The steady state solution for a weakly viscoelastic rotational thin film has a large leading order asymptotic Newtonian component. Therefore, the behavior observed largely resembles that of a Newtonian fluid (**Fig. 2(a)**). However, for more critical physical conditions (large q and De), the behavior diverges from that of a Newtonian fluid (**Fig. 2(b)**). To characterize this difference in behavior, the solutions' existence limits and relative uniformities are compared.

Leading order steady state solutions for various q are shown in **Fig. 3(a)**. The solutions exist for smaller values of $q < 2/3$, concentrating the thicknesses in puddles on the rising wall of the cylinder at θ=0. The thickness develops a shock in the form of a cusp on the rising wall when mass flux is raised to q=2/3 [13]. The steady state solution does not exist for values of $q > 2/3$; physically, this corresponds to the downward weight of the puddle being greater than the cylinder's upward rotational force, causing the puddle to descend down the cylinder wall.

The non-existence of the viscoelastic solution parallels that of the Newtonian (**Fig. 3(b)**). For a large q = 0.6665, the fluid develops zero and negative thickness at θ = 0. This is a nonphysical result, so the steady state solution fails to exist for this value and for those greater. Indeed, for q = 2/3, the solution develops a singularity at θ = 0, evident in both the figure and the denominator of the expression (72).

The source of this discontinuity could again be due to an imbalance of forces acting on the large mass of fluid. In this case, however, gravitational forces do not appear to work alone. For smaller q, the fluid's maximum value is below θ = 0, indicating gravitational influence on the puddle (**Fig. 3(b)**). But for larger q = 0.6542, the solution develops a saddle point, indicating the formation of a second maximum above θ = 0. This second maximum is evident for q = 0.664, and as the solution approaches the singularity, the second maximum becomes arbitrarily large. Evidence of a second maximum is counter-intuitive, since gravitational influence would force the puddle to slide down the wall. The second maximum can be attributed to the impact elastic forces acting on the fluid, since this type of film distribution cannot be obtained using the Newtonian model [25]. In pure numerical simulations [17], a similar maximum was also found above θ = 0 for viscoelastic rimming flow. This behavior is most likely caused by a combination of gravitational and viscoelastic forces compelling divergence of fluid downwards and upwards from θ = 0.

Upon examining the developing cusp in **Fig. 3(a)** and the negative-thickness singularity in **Fig. 3(b)**, it is apparent, since q < 2/3, that the viscoelastic solution **(b)** exhibits nonphysical behavior for smaller fluxes than the purely viscous **(a)**. This limitation is influenced by several factors related to the fluid's elasticity. In **Fig. 4(a)**, solutions of small De = 0.01, 0.1, and 0.2 exhibit physical behavior of $h(x) > 0$. After increasing De to 0.5, given the same q = 0.6666, the previously physical distribution becomes negative. Keeping De, the fluid's characteristic elasticity, small seems to allow for the solution to remain within the physical domain for this this magnitude of q. The elastic terms appear to contribute to the singular nature of the solution. Indeed, increasing K, the amount of viscous solvent in a viscoelastic polymeric solution, can raise the existence threshold for the viscoelastic solution as well, as seen in **Fig. 4(b)**. Clearly, in (72), raising K to 1 causes the viscoelastic thickness corrections to vanish.

A uniform thickness is ideal for industrial rimming flow. To quantify uniformity or lack thereof, the thickness-scaled variance, V, of a thin film thickness distribution, h, with viscoelastic parameters q, De, and K, is defined as:

$$V(q, De, K) = \frac{1}{2\pi \bar{h}} \int_{-\pi}^{\pi} (h(x) - \bar{h})^2 \, dx \tag{73}$$

where $\bar{h} = \frac{1}{2\pi} \int_{-\pi}^{\pi} h(x) dx$. Expanding solution (71) as a Taylor series of large accuracy $O(q^{70})$ with respect to small parameter $q \in [0, 2/3)$, the Newtonian variance, $V(q,0,0)$, is found to be a positive increasing function with one solution q = 0 for the equation $V(q, 0, 0) = 0$, evident in **Fig. 5** for De = 0. This shows that the Newtonian distribution is nearly constant for small q, but

becomes less uniform for increasing mass. This variance computation agrees with qualitative analysis given in [13]. An identical computation for *h(x)*, the viscoelastic distribution given by expressions (71) and (72), yields a different variance result (**Fig. 5**). The Newtonian and viscoelastic variances of mass flux *q* can be compared with the following computation:

$$\Delta(q, De, K) = V(q, De, K) - V(q,0,0) \tag{74}$$

By expanding *h(x)* as Taylor series with respect to *q*, Δ can be found for all $q \in [0, 2/3)$, $De \in [0, 1/2]$, and $K \in [0, 1]$. Our results, with Taylor series accuracy $O(q^{70})$, show that the inequality,

$$\Delta(q, De, K) \leq 0 \tag{75}$$

only has solutions {q = 0, De = 0, K = 1}, with $\Delta \geq 0$ for all investigated q, De, and K. Therefore, for nonzero elasticity and nonzero mass flux, a viscoelastic distribution shows greater deviation than a Newtonian film, evident in **Fig. 5**. When the elastic factors *De* and *K* are lowered, the viscoelastic variance, and as a result, Δ, lowers and approaches the purely viscous value. This suggests that elasticity lowers uniformity, and that polymeric solutes with weakly viscoelastic properties create slightly less uniform films than those without elastic properties.

In addition, the viscoelastic variance shares the property with that of the Newtonian in that, as $q \to 0$, $V \to 0$. In **Fig. 5**, as , as $q \to 0$ the viscoelastic variances asymptotically converge upon the Newtonian as they approach 0. For small mass flux *q*, a viscoelastic distribution is almost uniform.

7. Conclusions

Applying the Oldroyd-B model to viscoelastic rimming flow, the governing equations were derived in cylindrical coordinates. Scale analysis and asymptotic series expansion were implemented to obtain a simplified mathematical model.

The steady state thickness distributions were obtained for by removing time derivatives and solving the resulting equations analytically. The steady-state behavior was characterized. For non-zero *De*, as *q* increases, the film distribution becomes asymmetric (in contrast to Newtonian model) and its local maximum shifts down along the raising wall of the cylinder (below θ=0). For larger *q*, another local maximum is generated above θ=0. This is an unusual result, since a peak generation above zero would require overcoming gravitational forces.

The viscoelastic steady-state solution becomes physically meaningless for the smaller values of *q* than in in the case of Newtonian fluid, for which the upper limit is q=2/3. The viscoelastic solution develops negative thickness and a singularity for $q \to 2/3$. This limitation is likely due to elastic forces, since lowering characteristic elastic parameters *De* and *K* raises the threshold to Newtonian levels.

The elastic influences on steady-state behavior also had consequences on film uniformity. Using Taylor-expanded steady state solutions and a rescaled variance computation, the uniformity of the viscoelastic film was characterized. The solutions were found to be nearly uniform for small *q* and to become more uneven for larger *q*. The viscoelastic solution was found to be less uniform than that of the Newtonian for all nonzero *q*, *De*, and $K - 1$. Decreasing *De*

and increasing K reduced this differential, indicating that the elastic corrections to viscoelastic flow were responsible.

Acknowledgements

The authors would like to acknowledge the National Science Foundation for support of this project (NSF DMS Award #0648764).

Nomenclature

De	Deborah number
C_B	inverse to the Bond number
$\mathbf{D}$	rate of deformation tensor
$\mathbf{e}_r$, $\mathbf{e}_\theta$	radial and azimuthal axes vectors, respectively
$\mathbf{g}$	gravitational vector
H_0	mean thickness of the liquid layer
h	thickness of the liquid layer
h_0	characteristic thickness of the liquid layer
K	the ratio of the solvent viscosity to the solution viscosity
$\mathbf{n}$	normal to the free surface
p	pressure
q	mass flux
r	radial coordinate
r_o	radius of the cylinder
R	non-dimensional radial coordinate $= (1 - r) / \delta$
Re	Reynolds number as defined by equation
t	time
$\mathbf{v}$	fluid velocity
v_r, v_θ	radial and azimuthal components of the fluid velocity, respectively
W	total mass of the liquid
Greek symbols	
δ	ratio of the characteristic liquid layer thickness and radius of the cylinder (defined by equations (5))
κ	mean curvature of the free surface
λ_1	elastic relaxation time
λ_2	elastic retardation time
μ	dynamic viscosity
θ	azimuthal coordinate
ρ	liquid density
σ	surface tension
$\boldsymbol{\tau}$	stress tensor

$\tau_{\theta R}$, τ_{RR}, $\tau_{\theta\theta}$ components of $\boldsymbol{\tau}$

Ω angular velocity of the cylinder

Superscripts

* dimensional quantities

0,1 zero-order and first-order approximation, respectively

Subscripts

0 characteristic quantity (excluding h_0 and h_1)

θ, *r* azimuthal and radial components, respectively

Vector and Tensor Notation & Operations

s scalar (lightface italic)

v vector (boldface italic)

$\boldsymbol{\tau}$ second-order tensor (boldface Greek)

( ) scalar

[ ] vector

{} tensor

$\nabla\mathbf{v}$ dyadic product (tensor)

$\nabla\cdot\mathbf{v}$ inner product

Displacement Gradient Tensor in Cylindrical Coordinates

$$\nabla\mathbf{v}=\begin{bmatrix}\dfrac{\partial v_r}{\partial r} & \dfrac{1}{r}\left(\dfrac{\partial v_r}{\partial\theta}-v_\theta\right)\\ \dfrac{\partial v_\theta}{\partial r} & \dfrac{1}{r}\left(\dfrac{\partial v_\theta}{\partial\theta}+v_r\right)\end{bmatrix}$$

Deformation Rate Tensor

$$\mathbf{D}=\frac{1}{2}\left(\nabla\mathbf{v}+(\nabla\mathbf{v})^T\right)$$

References

[1] Harkin-Jones, E., and Crawford, R.J. Rotational moulding of liquid polymers. In: *Rotational Moulding of Plastics* (R.J. Crawford ed.), J. Wiley, New York, (1996) 243–255.

[2] Throne J. L. and Gianchandani J., Reactive rotational molding**,** *Polymer Engineering & Science*, **20** (13) (1980) 899-919

[3] Moffatt, H.K., Behavior of viscous film on the surface of a rotating cylinder, *J. Mecanique* **16** (1977) 651-673

[4] Preziosi, L. and Joseph, D.D., The Run-Off Condition for Coating and Rimming Flows, *J. Fluid. Mech.*, **187**, (1988) 99-113.

[5] Benilov, E.S. and O'Brien, S.B.G., Inertial instability of a liquid film inside a rotating horizontal cylinder. *Phys. Fluids*. **17**, (2005) 052106.
[6] Benilov, E.S. Explosive instability in a linear system with neutrally stable eigenmodes. Part 2: Multi-dimensional disturbances. *J. Fluid Mech*. **501**, (2004) 105-124.
[7] Benilov, E.S., Lacey, S.M. and O'Brien, S. B. G., Exploding solutions for three-dimensional rimming flows. *Q. J. Mech. Appl. Math.* **58**, (2005), 563-576.
[8] Benilov, E.S., O'Brien, S.B.G., and Sazonov, I. A., A new type of instability: explosive disturbances in a liquid .lm inside a rotating horizontal cylinder. *J. Fluid Mech*. **497**, (2003) 201-224.
[9] Johnson, R.E., Coating flow stability in rotating molding, in .Engineering Science, *Fluid Dynamics*: A symposium to Honor Wu T. Y., World Scientific, (1990) 435-449.
[10] Villegas-Diaz, M., Power, H., and Riley, D.S., Analytical and numerical studies of the stability of thin-film rimming flow subject to surface shear. *J. Fluid Mech*. **541**, (2005) 317-344.
[11] Fomin, S., Kilpatrick, K. and Hubbard, R., Rimming Flow of a Power-Law Fluid: Qualitative Analysis of the Mathematical Model and Analytical Solutions, *Applied Mathematics and Computation*, vol. **216**, 2010, pp. 2169-2176.
[12] Johnson, R.E., Steady-State Coating Flows Inside a Rotating Horizontal Cylinder, *J. Fluid. Mech.*, **190**, (1988) 321-342.
[13] Fomin, S., Watterson, J., Raghunathan, S. and Harkin-Jones, E., Steady-State Rimming Flow of the Generalized Newtonian Fluid, *Physics of Fluids*, **14** (9) , (2002) 3350-3353.
[14] Fomin, S., Hashida, T. and Watterson, J., Fundamentals of steady-state non-Newtonian rimming flow, *J. non-Newtonian Fluid Mech*.**111** (2003) 19-40.
[15] Fomin, S., "Three Regimes of Non-Newtonian Rimming Flow", *ASME Journal of Fluids Engineering*, **128**, (2006), 107-112
[16] Ross, A. B., Wilson, S.K. and Duffy, B.R., Thin-film flow of a viscoplastic material round a large horizontal stationary or rotating cylinder, *J. Fluid Mech*. **430** (2001) 309-333.
[17] Rajagopalan, D., Phillips, R., Armstrong, R., Brown, R. and Bose, A., The influence of viscoelasticity on the existence of steady solutions in two-dimensional rimming flow, *J. Fluid Mech.* **235** (1992) 611-642.
[18] Fomin, S., Debrunner, J., Mazurenko, A. and Nelson, B., Steady state visco-elastic rimming flow, *Applied Mathematical Modeling* **35** (2011) 1846-1860.
[19] Lawrence, C.J. and Zhou, W., Spin coating of non-Newtonian fluids, *J. Non-Newtonian Fluid Mech.* **39** (1991) 137-187.
[20] Jenekhe, S.A. and Schuldt, S.B., Coating of non-Newtonian fluids on a flat rotating disk, *Ind. Engng. Chem. Fundam.* **23** (1984) 432-436.
[21] Bird, R.B., Armstrong, R.C., and Hassager, O., Dynamics of Polymeric Liquids, Vol.1, *Fluid Dynamics*, Willey, New York, 1977.
[22] Khayat, R. E. and Kim, K.-T., Thin-film flow of a viscoelastic fluid on an axisymmetric substrate of arbitrary shape, *J. Fluid Mech*., **552** (2006), 37-71.

[23] Boyd, J. P., Hyperasymptotics and the Linear Boundary Problem: Why Asymptotic Series Diverge, , *SIAM Review*, **47**, No. 3 (2005) 553-575
[24] O'Brien, S. B. G. and Gath, E. G., The location of a shock in rimming flow, *Phys. Fluids* **10** (1998) 1040-1042.
[25] Melo, F., Localized states in film-dragging experiments, *Phys. Rev. E.* **48** (1993) 2704-2712.
[26] LaSalle, J. and Lefschetz, S. *Stability by Lyapunov's direct method with applications.* Academic Press, New York (1961). vii + 133 pp.

Figures and captions

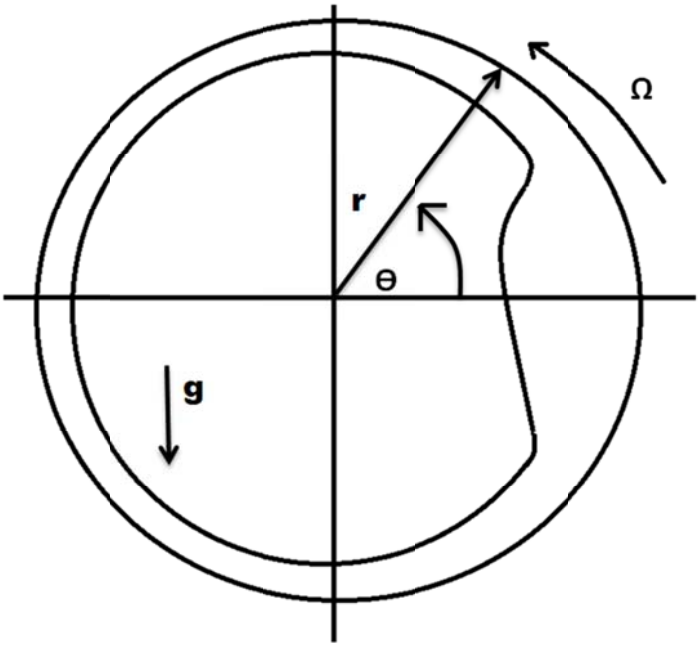

Fig. 1: A schematic sketch of viscoelastic rimming flow on the wall of a horizontal, rotating cylinder. Notice the presence of a peak above the horizontal plane.

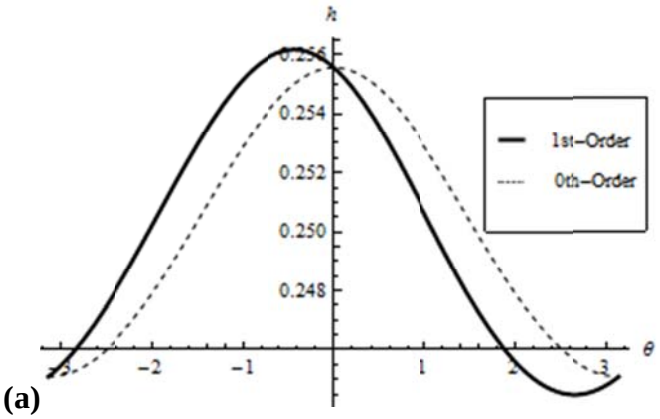

(a)

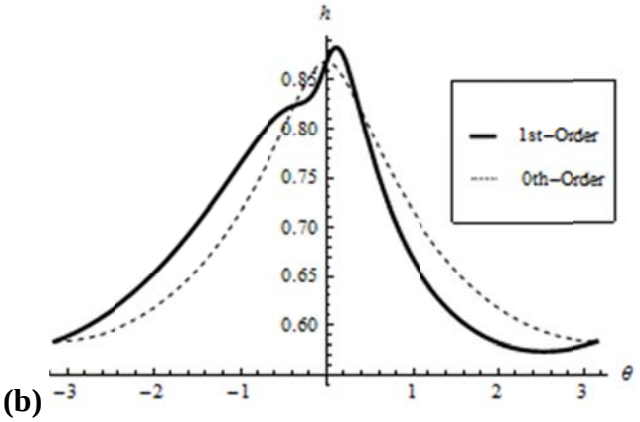

(b)

Fig. 2: leading (*De* = 0) and 1st order *(De = ½)* approximations of viscoelastic behavior for *K* = 0. **(a)** is for smaller mass flux *q* = 0.3, **(b)** is for larger *q* = 0.6542.

.

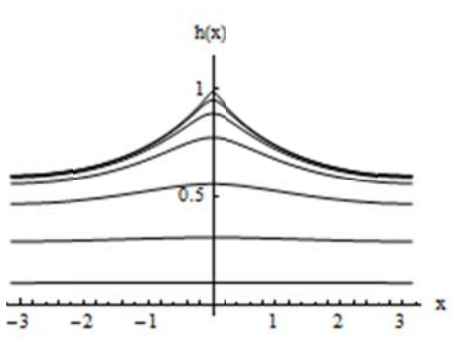

(a)

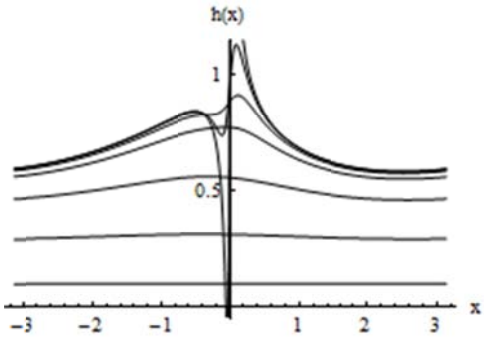

(b)

Fig. 3: leading and 1st order approximations for viscoelastic fluid thickness for various *q* = 0.1, 0.3, 0.5, 0.62, 0.6542, 0.664, and 0.6665, with *K* = 0. **(a)** depicts the leading order for *De* = 0, **(b)** depicts the 1st order for *De* = ½.

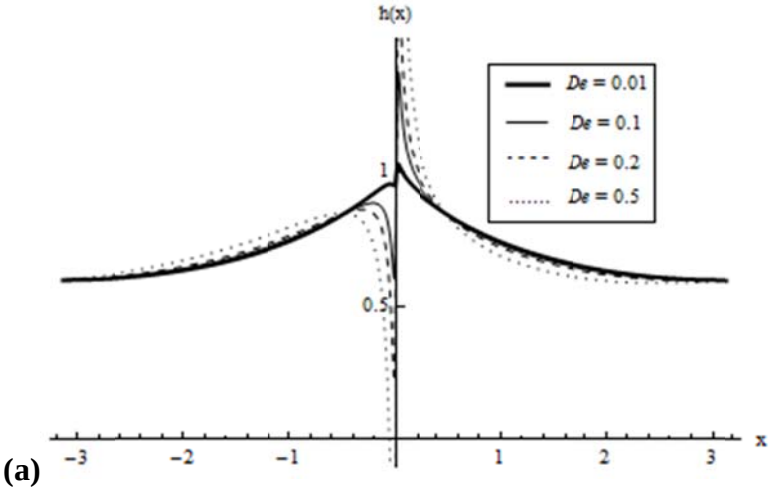

(a)

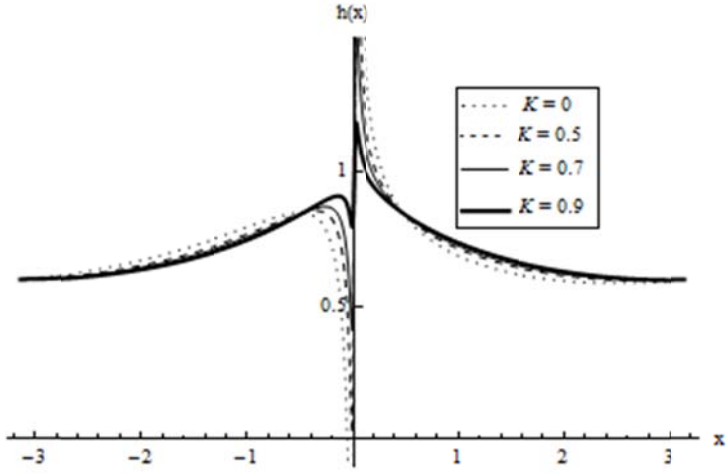

(b)

Fig. 4: Viscoelastic distributions of $q = 0.6666$ for different elastic values. **(a)** is for different De with $K = 0$, **(b)** is for $De = 0.5$ with different K.

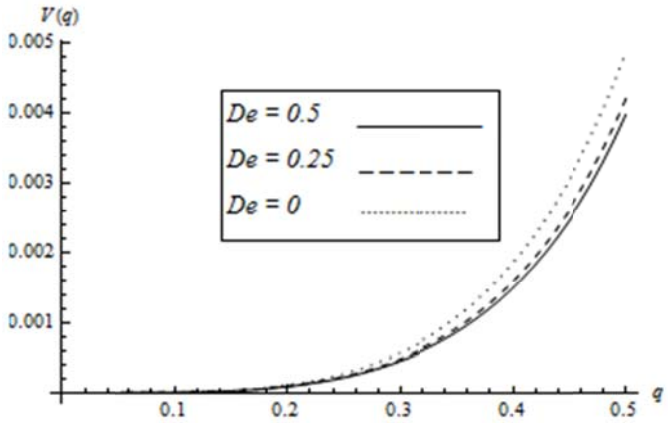

Fig. 5: Thickness variance $V(q)$ for $K = 0$ and various De.